Polyhedron 29 (2010) 100–109

Contents lists available at ScienceDirect

Polyhedron

journal homepage: www.elsevier.com/locate/poly

Halo and azido copper(II) coordination polymers featuring the *gem*-diolate forms of di-2-pyridyl ketone

Harikleia Sartzi [a], Giannis S. Papaefstathiou [b], Vassilis Psycharis [c], Albert Escuer [d], Spyros P. Perlepes [a], Constantinos C. Stoumpos [a,d,*]

[a] Department of Chemistry, University of Patras, 26504 Patras, Greece
[b] Laboratory of Inorganic Chemistry, Department of Chemistry, National and Kapodistrian University of Athens, Panepistimiopolis, 15771 Zografou, Greece
[c] Institute of Materials Science, NCSR "Demokritos", 15310 Aghia Paraskevi Attikis, Athens, Greece
[d] Departament de Quimica Inorganica, Universitat de Barcelona, Diagonal 647, 08028 Barcelona, Spain

ARTICLE INFO

Article history:
Available online 11 June 2009

Keywords:
Copper(II) complexes
Crystal structures
Di-2-pyridyl ketone
Magnetic properties
One-dimensional coordination polymers

ABSTRACT

The reactions of di-2-pyridyl ketone, $(py)_2CO$, with $[Cu_2(O_2CMe)_4(H_2O)_2]$ in the presence of NaN_3, HCl and HBr have led to the isolation of complexes $\{[Cu_8\{(py)_2CO_2\}_4(N_3)_6(O_2CMe)_2]\cdot 2MeCN\cdot H_2O\}_\infty$ (**1**·2MeCN·H_2O), $[Cu_2\{(py)_2C(OH)O\}Cl_3]_\infty$ (**2**) and $[Cu_2\{(py)_2C(OH)O\}Br_3]_\infty$ (**3**), respectively, where $(py)_2CO_2^{2-}$ and $(py)_2C(OH)O^-$ are the dianion and the monoanion of the *gem*-diol form of $(py)_2CO$. Complex **1**·2MeCN·H_2O is an 1D coordination polymer consisting of centrosymmetric $[Cu_8\{(py)_2CO_2\}_4(N_3)_6(O_2CMe)_2]$ cluster units linked through weakly coordinated azido bridges. The $(py)_2CO_2^{2-}$ groups adopt the $\eta^1{:}\eta^2{:}\eta^2{:}\eta^1{:}\mu_4$ coordination mode, while the N_3^- ions behave as $\eta^2{:}\mu$ and $\eta^1{:}\ \eta^2{:}\mu_3$ ligands. The isostructural compounds **2** and **3** are also 1D coordination polymers consisting of $\{Cu_2\{(py)_2C(OH)O\}X_3\}_2$ units (X=Cl, Br) linked through double halo bridges. The $(py)_2C(OH)O^-$ ligand adopts the tridentate, bis-chelating $\eta^1{:}\eta^2{:}\ \eta^1{:}\mu$ mode. A common feature in the three complexes is the presence of *interchain* H-bonding interactions which result in the formation of 2D networks. The magnetic properties of **1**–**3** have been studied by variable-temperature dc magnetic susceptibility and variable-field magnetization techniques. The analyses of the magnetic data were performed taking into account only the dominant exchange interactions within dinuclear subunits. The intradinuclear exchange interactions have been found to vary from strongly and moderately antiferromagnetic in **1** to ferromagnetic in **2** and **3**. This work demonstrates the flexibility, versatility and synthetic potential of combining $(py)_2CO$ with carboxylate and azido or halo ligands.

1. Introduction

The coordination chemistry of Cu^{II} has been significantly developed in the last four decades for a variety of reasons. From the bioinorganic chemistry viewpoint, the modeling of active sites in Cu biomolecules has been pursued [1], while from the magnetochemistry viewpoint dinuclear complexes have been synthesized in order to create magnetostructural correlations [2] and trinuclear complexes have attracted interest in order to study spin frustration and antisymmetric exchange phenomena [3], as well as for the rational synthesis of ferromagnetic entities [4]. Infinite lattices constitute another well-studied class of Cu^{II} compounds leading to construction of 1D, 2D and 3D architectures [5], while Cu^{II} polymetallic complexes with esthetically pleasing structures and interesting magnetic properties are also a "hot" topic in contemporary coordination chemistry [6].

Our interest focuses on the synthesis of polymetallic Cu^{II} complexes using di-2-pyridyl ketone, $(py)_2CO$ (Scheme 1), as an organic ligand. The special characteristic of this organic molecule is the susceptibility of its ketone group towards nucleophilic attack. Several nucleophiles have been used aiming at the *in situ* transformation of the $(py)_2CO$ ligand, but H_2O is by far the most interesting nucleophile since it produces the *gem*-diolate (−1 or −2) forms of the ligand (Scheme 1) which have increased potential for the assembly of polynuclear species compared with other nucleophile-based, transformed derivatives of the ligand. The Cu^{II} chemistry of $(py)_2CO$ is already well studied having produced Cu_2 [7], Cu_4 [8], Cu_6 [9], Cu_7 [10], Cu_8 [11], Cu_{11} [12] and Cu_{12} [10] polynuclear species featuring the *gem*-diolate forms $(py)_2C(OH)O^-$ and $(py)_2CO_2^{2-}$ and some polymeric species based on polymerization of discrete $\{Cu_2\}$ subunits [13]. Compounds bearing the hemiketalate form of the ligand have also been reported, but these compounds are limited to Cu_2 [14], Cu_4 [15] and polymeric species

* Corresponding author. Address: Department of Chemistry, University of Patras, 26504 Patras, Greece. Tel.: +30 2610 996019; fax: +30 2610 997118.
E-mail address: kstoump@upatras.gr (C.C. Stoumpos).

0277-5387/$ - see front matter © 2009 Elsevier Ltd. All rights reserved.
doi:10.1016/j.poly.2009.06.016

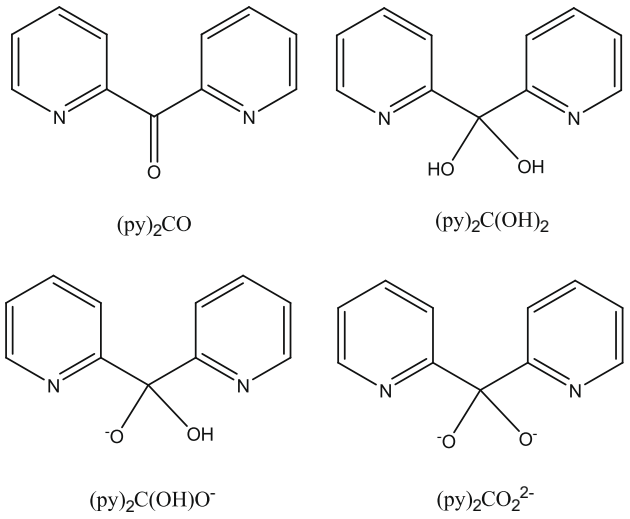

Scheme 1. The di-2-pyridyl ketone ligand and its neutral, singly and doubly deprotonated *gem*-diol forms. Note that $(py)_2C(OH)_2$, $(py)_2C(OH)O^-$ and $(py)_2CO_2^{2-}$ do not exist as free species but they exist only in the presence of metal ions.

[16], a clear indication that the extra donor atom of the *gem*-diolate forms makes di-2-pyridyl ketone an excellent ligand for the exploration of reaction pathways that might lead to polynuclear complexes. This statement is also supported by the behavior of this ligand towards other metal ions [17]. This report describes the preparation and characterization of three Cu^{II} coordination polymers possessing *both* azido (N_3^-) or halo (Cl^-, Br^-) ions and *gem*-diolate forms of $(py)_2CO$ as ligands.

2. Experimental

2.1. General and physical measurements

All manipulations were performed under aerobic conditions using materials (reagent grade) and solvents as received. Elemental analyses (C, H, N) were performed by the University of Ioannina (Greece) Microanalytical Laboratory using an EA 1108 Carlo Erba analyzer. IR spectra (4400–450 cm^{-1}) were recorded as KBr pellets on a Perkin–Elmer 16 PC spectrometer. Variable-temperature, solid-state direct current (dc) magnetic susceptibility data down to 2.0 K were collected on a Quantum Design MPMS-XL SQUID magnetometer at the Magnetochemistry Service of the University of Barcelona. Diamagnetic corrections were applied to the observed paramagnetic susceptibilities using Pascal's constants.

2.2. Preparation of the compounds

2.2.1. $\{[Cu_8\{(py)_2CO_2\}_4(N_3)_6(O_2CMe)_2]\cdot 2\,MeCN\cdot H_2O\}_\infty$ (**1**·2MeCN·H_2O)

To a stirred blue solution containing $[Cu_2(O_2CMe)_4(H_2O)_2]$ (0.6 mmol, 240 mg), $(py)_2CO$ (0.6 mmol, 110 mg) and Et_3N (1.2 mmol, 166 μl) in MeCN (20 ml) was added an aqueous solution (4 ml) of NaN_3 (0.6 mmol, 39 mg). No significant color change was observed and stirring was continued for a further 30 min. Slow evaporation of the solvent at room temperature led to X-ray quality, blue-green crystals of the product after 2 days. The yield was ~50% based on NaN_3. *Anal.* Calc. for $C_{52}H_{46}Cu_8N_{28}O_{13}$: C, 35.10; H, 2.61; N, 22.04. Found: C, 35.47, H, 2.55; N, 22.13%. IR (KBr pellet, cm^{-1}): 3421 mb, 3024 w, 2959 w, 2057 m, 1584 s, 1560 s, 1481 m, 1438 m, 1406 s, 1340 m, 1300 w, 1234 m, 1161 w, 1129 w, 1109 w, 1065 m, 1045 s, 965 w, 814 w, 770 m, 702 m, 686 m, 670 m, 653 m, 617 w, 529 m, 466 w.

2.2.2. $[Cu_2\{(py)_2C(OH)O\}Cl_3]_\infty$ (**2**)

A deep blue solution of $[Cu_2(O_2CMe)_4(H_2O)_2]$ (0.3 mmol, 120 mg) and $(py)_2CO$ (0.3 mmol, 55 mg) in MeCN was treated with an aqueous 1 M HCl solution (1.2 mmol, 1.2 ml). The color of the solution changed immediately to deep green. Subsequent slow evaporation of the solvent yielded green crystals of **2** after 2 days. The yield was 30%. *Anal.* Calc. for $C_{11}H_9Cl_3Cu_2N_2O_2$: C, 30.40; H, 2.09; N, 6.45. Found: C, 30.52, H, 2.05; N, 6.51. IR (KBr pellet, cm^{-1}): 3475mb, 3118 w, 3094 w, 2925 m, 1604 m, 1570 m, 1559 m, 1473 m, 1441 m, 1346 m, 1290 w, 1230 m, 1199 m, 1173 m, 1130 m, 1076 vs, 1066 vs, 1038 vs, 951 m, 903 w, 800s, 774s, 767 s, 745 m, 689 m, 667 m, 653 m, 623 w, 561 w, 494 w.

2.2.3. $[Cu_2\{(py)_2C(OH)O\}Br_3]_\infty$ (**3**)

A synthetic process similar to that employed for compound **2** was employed, replacing HCl with HBr. The yield was 20%. *Anal.* Calc. for $C_{11}H_9Br_3Cu_2N_2O_2$: C, 23.26; H, 1.60; N, 4.93. Found: C, 23.47, H, 1.55; N, 4.99%. IR (KBr pellet, cm^{-1}): 3466 mb, 3115 w, 3096 w, 2915 m, 1600 m, 1570 m, 1557 m, 1476 m, 1442 m, 1343 m, 1293 w, 1232 m, 1199 m, 1173 m, 1129 m, 1079 vs, 1060 vs, 1042 vs, 951 m, 903 w, 802s, 776s, 770 s, 744 m, 690 m, 666 m, 653 m, 561 w, 494 w.

2.3. Crystal structure determination

A bluish green crystal of **2** (0.06 × 0.17 × 0.65 mm) was mounted in air, while green crystals of **1**·2MeCN·H_2O (0.10 × 0.10 × 0.20 mm) and **3** (0.07 × 0.14 × 0.29 mm) were taken directly from the mother liquor and immediately cooled to −93 °C. Diffraction measurements were made on a Rigaku R-AXIS SPIDER Image Plate diffractometer using graphite monochromated Cu Kα (for **2**) or Mo Kα (for **1**·2MeCN·H_2O and **3**) radiations. Data collection (ω-scans) and processing (cell refinement, data reduction and empirical absorption correction) were performed using the CRYSTALCLEAR program package [18]. Important crystallographic and refinement data are listed in Table 1. The structures were solved by direct methods using SHELXS-97 [19] and refined by full-matrix least-squares techniques on F^2 with SHELXL-97 [20]. Further crystallographic details for **2**: $2\theta_{max} = 130°$; 217 parameters refined; $(\Delta/\sigma)_{max} = 0.001$; R/R_w (for all data), 0.0287/0.0744. Hydrogen atoms were located by difference maps and were refined isotropically. All non-H atoms were refined anisotropically. Further crystallographic details for **1**·2MeCN·H_2O: $2\theta_{max} = 52°$; 525 parameters refined; $(\Delta/\sigma)_{max} = 0.005$; R/R_w (for all data), 0.0440/0.0754. Hydrogen atoms were located by difference maps and were refined isotropically. All non-H atoms were refined anisotropically. Further crystallographic details for **3**: $2\theta_{max} = 54°$; 217 parameters refined; $(\Delta/\sigma)_{max} = 0.001$; R/R_w (for all data), 0.0262/0.0497. Hydrogen atoms were located by difference maps and were refined isotropically. All non-H atoms were refined anisotropically.

3. Results and discussion

3.1. Syntheses

The investigation of the $[Cu_2(O_2CMe)_4(H_2O)_2]/(py)_2CO$ in MeCN reaction system is known in MeCN to produce a mixture of heptanuclear and dodecanuclear Cu^{II} compounds [10]. This work represents an expansion of the previous work; our plan was to study the reactivity of these compounds in basic or acidic environment in the presence of halide or azide ligands, following our previous efforts on $Mn(O_2CR)_2/(py)_2CO$ reaction system, where tetranuclear Mn^{II} species were efficiently converted to tetradecanuclear mixed-valent Mn clusters [21]. We favored the base- and acid-mediated reactions as a means to separate the mixtures of the $[Cu_7(OH)_2$

Table 1
Crystallographic data for complexes **1**.MeCN·2H_2O, **2** and **3**.

Parameter	**1**·2MeCN·H_2O	**2**	**3**
Formula[a]	$C_{52}H_{46}Cu_8N_{28}O_{13}$	$C_{11}H_9Cl_3Cu_2N_2O_2$	$C_{11}H_9Br_3Cu_2N_2O_2$
M	1779.48	434.63	568.02
Crystal size (mm)	0.10 × 0.10 × 0.20	0.06 × 0.17 × 0.65	0.07 × 0.14 × 0.29
Crystal system	triclinic	triclinic	triclinic
Space group	$P\bar{1}$	$P\bar{1}$	$P\bar{1}$
a (Å)	10.631(1)	8.533(1)	8.784(1)
b (Å)	11.995(1)	9.403(0)	9.620(1)
c (Å)	14.296(1)	10.238(1)	10.223(1)
α (°)	82.97(1)	73.88(1)	73.77(1)
β (°)	67.05(1)	71.13(1)	70.82(1)
γ (°)	74.50(1)	64.31(1)	63.99(1)
V (Å^3)	1617.3(1)	691.3(1)	723.9(1)
Z	1	2	2
T (K)	180(2)	298(2)	180(2)
$2\theta_{max}$ (°)	52.00	129.86	54.00
λ (Å)	0.71073[b]	1.54187[c]	0.71073[b]
ρ_{calc} (g cm^{-3})	1.827	2.088	2.606
μ (mm^{-1})	2.661	9.145	11.216
Measd/independent reflns (R_{int})	34377/6344(0.0457)	7788/2072(0.0353)	16816/3145(0.0457)
Observed reflections [$I > 2\sigma(I)$]	5177	1967	2825
R_1[d]	0.0311	0.0274	0.0218
wR_2[e]	0.0704	0.0736	0.0476
Goodness of Fit (GoF) on F^2	1.031	1.090	1.084
$(\Delta\rho)_{max,min}$ (e Å^{-3})	0.435, −0.435	0.410, −0.472	0.489, −0.581

[a] Including solvate molecules.
[b] Mo Kα radiation, graphite monochromator.
[c] Cu Kα radiation, graphite monochromator.
[d] $R_1 = \sum(|F_o| - |F_c|)/\sum(|F_o|)$ for observed reflections.
[e] $wR_2 = \{\sum[w(F_o^2 - F_c^2)^2]/\sum[w(F_c^2)^2]\}^{1/2}$ for observed reflections.

$\{(py)_2CO_2\}_3(O_2CMe)_6]$ and $[Cu_{12}\{(py)_2CO_2\}_6(O_2CMe)_{12}]$ products, taking advantage of the presence and the absence of OH^- ligands in the heptanuclear and dodecanuclear clusters, respectively. Thus, the presence of basic conditions would favor the formation of the Cu_7 species, whereas acidic conditions would tip the balance towards the formation of the Cu_{12} species. This turned out to be the case and in fact we have isolated a series of heptanuclear and dodecanuclear species [22]. During these synthetic attempts we found out that the nature of the acid or base present plays a major role in the identity of the final product and in fact has led to some non-Cu_7 and non-Cu_{12} complexes which are the "by-products" of the aforementioned general reaction system.

The $[Cu_2(O_2CMe)_4(H_2O)_2]$/$(py)_2CO$/Et_3N/NaN_3 reaction system in MeCN afforded the polymeric compound $[Cu^{II}_8\{(py)_2CO_2\}_4(N_3)_6(O_2CMe)_2]_\infty$ (**1**) which is based on octanuclear Cu^{II} clusters units. The initial concept was that by using the N_3^- ligands in a reaction system that favors the Cu_7 cluster, we would be able to realize the replacement of the hydroxo bridges by end-on azido ligands, as it has been reported for M^{II}_9 (M = Fe, Co, Ni) clusters featuring the doubly deprotonated *gem*-diolate form of di-2-pyridyl ketone, $(py)_2CO_2^{2-}$ [23]. We felt that the structural "similarity" of the Cu_7 and M_9 compounds (in the sense that the μ_3–OH^- defines a Cu_3 triangle in the Cu^{II}_7 cluster, whereas the μ_4–OH^- defines a M_4 square in the M^{II}_9 clusters) would lead to similar chemical behavior. This turned out to be just a speculation since crystallographic evidence revealed that the Cu_7 core completely dissociates in the presence of N_3^- anions towards formation of azido-bridged octanuclear cluster units. Attempts to isolate different products by varying the NaN_3:Cu^{II} ratio failed, since reducing the NaN_3 quantity yielded the $[Cu_7(OH)_2\{(py)_2CO_2\}_3(O_2CMe)_6]$ cluster, whereas an increase of the ratio led to non-crystalline, py_2CO-free solids. Moreover, attempts to change the nature of the pseudohalide ligand by using SCN^- or OCN^- sources did not lead to structurally characterisable products.

Reactions of $[Cu_2(O_2CMe)_4(H_2O)_2]$ with py_2CO in the presence of HX (X = Cl, Br) in MeCN led to the formation of complexes $[Cu^{II}_2\{(py)_2C(OH)O\}X_3]_\infty$ (**2**, X = Cl^-; **3**, X = Br^-). The initial target for the study of this reaction system was the selective isolation of $[Cu_{12}\{(py)_2CO_2\}_6(O_2CMe)_{12}]$ over $[Cu_7(OH)_2\{(py)_2CO_2\}_3(O_2CMe)_6]$ by eliminating the OH^- species responsible for the formation of the latter complex. However, the effect of the halide ions dominates over the acetate ions in solution, leading to the formation of Cu^{II} halide species, the presence of which is evident by the spontaneous color change from deep blue to deep green, observed after the addition of HX in the reaction mixture. The reaction proceeds equally well with both Cl^- and Br^- ligands, but I^- definitely follows a different pathway leading to dark red colored solutions, probably involving formation of Cu^I-containing species; unfortunately, the quality of the gray crystalline solid that we isolated was insufficient for crystal structure determination. Although we did not investigate the effect of HF in the reaction mixture, a recent study [24] of a similar reaction system revealed the presence of mononuclear $[Cu\{(py)_2C(OH)_2\}_2](H_2F_3)_2$ species featuring the "exotic" $H_2F_3^-$ counteranions.

3.2. Description of structures

Aspects of the molecular structure of $[Cu_8\{(py)_2CO_2\}_4(N_3)_6(O_2CMe)_2]_\infty$ (**1**) are depicted in Fig. 1, while selected interatomic distances and angles are listed in Table 2.

Complex **1** is an 1D coordination polymer consisting of centrosymmetric $[Cu^{II}_8\{(py)_2CO_2\}_4(N_3)_6(O_2CMe)_2]$ units linked through weakly coordinated azido bridges. The crystallographically independent unit, $\{Cu_4\{(py)_2CO_2\}_2(N_3)_3(O_2CMe)\}$, consists of four Cu^{II} ions, two doubly deprotonated $(py)_2CO_2^{2-}$, three azide and one acetate ligands. All four Cu^{II} ions are surrounded by four donor atoms in the equatorial/basal plane through strong coordination bonds (1.93–2.01 Å). In two of the Cu^{II} ions [Cu(2) and Cu(3)] there is a fifth donor atom on an axial position, moderately [in Cu(2)] or weakly [in Cu(3)] coordinated to the metal and defining the apex of a square pyramidal geometry. The other two Cu^{II} ions [Cu(1) and Cu(4)] are surrounded by two weakly coordinated donor atoms in axial

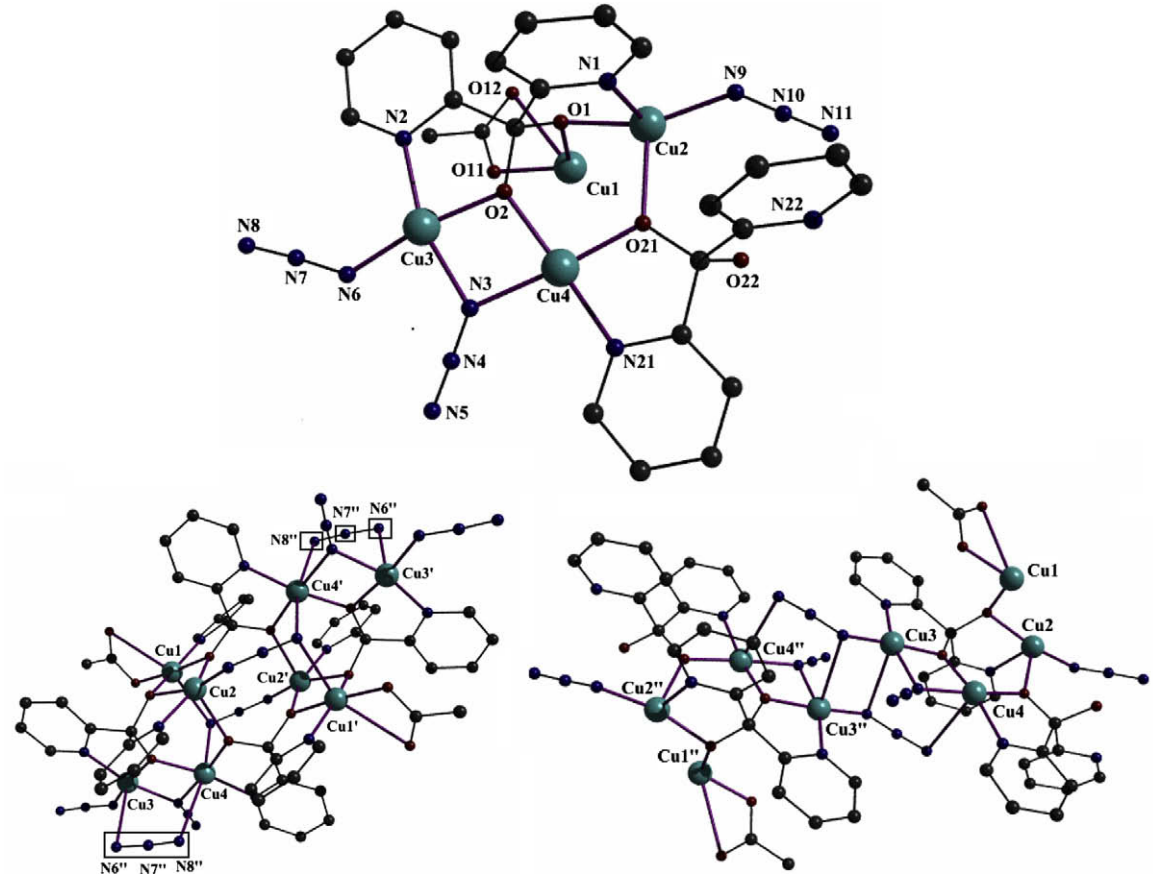

Fig. 1. The structure of the crystallographically independent, $\{Cu_4\{(py)_2CO_2\}_2(N_3)_3(O_2CMe)\}$ repeating unit (top) present in compound **1**·2MeCN·H_2O. The head-to-head (bottom left) and tail-to-tail (bottom right) linkages of two, crystallographically independent repeating units resulting in the formation of a discrete $[Cu_8\{(py)_2CO_2\}_4(N_3)_6(O_2CMe)_2]$ molecular cluster unit (left) and a weakly bonded $\{Cu_4\{(py)_2CO_2\}_2(N_3)_3(O_2CMe)\}_2$ dimeric unit (right). The coordination environment around the Cu^{II} ions is complete only in the picture of $[Cu_8\{(py)_2CO_2\}_4(N_3)_6(O_2CMe)_2]$, in which the boxed nitrogen atoms [N(6″),N(7″),N(8″)] belong to weakly bonded, adjacent $[Cu_8\{(py)_2CO_2\}_4(N_3)_6(O_2CMe)_2]$ units. H atoms and solvate molecules are omitted for clarity.

position along the Jahn–Teller axis defining an elongated octahedral geometry around the metal centers. The coordination environment varies with Cu(1), Cu(2), Cu(3) and Cu(4); the coordination spheres are CuO_4N_2, CuO_3N_2, $CuON_4$ and CuO_2N_4, respectively.

The assembly of the coordination polymer is achieved through repetition of the tetranuclear $\{Cu_4\{(py)_2CO_2\}_2(N_3)_3(O_2CMe)\}$ subunit through head-to-head and tail-to-tail linkages. As head-to-head linkage we define the centrosymmetric connection between the Cu(1)Cu(2)Cu(4) and Cu(1′)Cu(2′)Cu(4′) triangular arrays, see bottom left of Fig. 1. The connection is achieved through two azido and two $py_2CO_2^{2-}$ ligands. Through this linkage the octanuclear cluster unit $[Cu^{II}_8\{(py)_2CO_2\}_4(N_3)_6(O_2CMe)_2]$ assembles. The tail-to-tail connection is also centrosymmetric and occurs between the Cu(3)Cu(4) and Cu(3′)Cu(4′) pairs, see bottom right of Fig. 1. The connection is achieved through two azido ligands. Through this weak linkage [Cu–N = 2.906(3) and 2.943(3) Å] the $\{Cu_8\}$ units are further connected towards formation of infinite molecular chains of octanuclear cluster units (Fig. 2).

The $(py)_2CO_2^{2-}$ crystallographically independent ligands have a dual role; first, they hold together all the four Cu^{II} ions within the tetranuclear moiety, which can be considered as the primary building block, and second, they act as linkers between two tetranuclear units ultimately assembling the secondary building block, the octanuclear cluster unit $[Cu_8\{(py)_2CO_2\}_4(N_3)_6(O_2CMe)_2]$. The $\eta^1{:}\eta^2{:}\eta^2{:}\eta^1{:}\mu_4$ coordination mode of the doubly deprotonated ligand which is adopted in complex **1** (Scheme 2) is the most common in Cu^{II} clusters, already reported in Cu_6 [9], Cu_8 [11], Cu_{11} [12] and Cu_{12} [10] complexes. The azido ligands in complex **1** adopt exclusively bridging coordination modes. The N(3)N(4)N(5) ion bridges Cu(3) and Cu(4) monoatomically through N(3) [$\eta^2{:}\mu$], see Scheme 2. The other two, crystallographically independent N_3^- ions bridge in the rare $\eta^1{:}\eta^2{:}\mu_3$ mode, with N(6) and N(9) strongly coordinated to Cu(3) and Cu(2), respectively; atom N(11) forms two weak bonds [2.478, 2.567 Å] to Cu(1′) and Cu(2′), while the interactions of N(6) and N(8) to Cu(3″) and Cu(4″), respectively, are both very weak [2.906, 2.943 Å], see Scheme 2. The terminally bound, (pseudo)chelating acetate ligand [Cu–O = 1.932, 2.809 Å] is not involved in the polymerization along the chain, but it is H-bonded to the solvate H_2O molecule (this molecule is disordered over two positions with 50% occupancy) which in turn acts as a linker between two neighboring chains creating a 2D network through supramolecular interactions (vide infra).

Aspects of the molecule structures of complexes **2** and **3** are depicted in Fig. 3, while interatomic distances and angles are listed in Table 3. Since the molecular structure of the two complexes is essentially the same, only the structure of complex **2** will be described in detail.

Complex **2** is an 1D coordination polymer consisting of crystallographically independent $\{Cu_2\{py\}_2C(OH)O\}Cl_3\}$ units, see top of Fig. 3. Each of the Cu^{II} ions in the dinuclear moiety is 5-coordinate featuring a $NOCl_3$ coordination sphere. The coordination geometry of both metal centers is distorted square pyramidal; the apical positions are occupied by Cl^- ions that belong to neighboring dinuclear units.

The propagation of the polymer is achieved through double, centrosymmetric chloro bridges that bind to Cu(2) and Cu(2′)

Table 2
Selected interatomic parameters for **1**·2MeCN·H_2O. Distances and angles are given in (Å) and (°), respectively.[a]

Cu(1)–O(1)	1.944(2)	Cu(4)–O(21)	1.910(2)
Cu(1)–O(11)	1.932(2)	Cu(4)–N(3)	2.011(3)
Cu(1)–O(12)	2.809(3)	Cu(4)–N(21)	1.985(2)
Cu(1)–O(22′)	1.931(2)	Cu(4)–N(8″)	2.943(3)
Cu(1)–N(11′)	2.567(3)	Cu(4)–N(11′)	2.478(3)
Cu(1)–N(22′)	1.986(3)	Cu(1)···Cu(2)	2.990(1)
Cu(2)–O(1)	1.970(2)	Cu(1)···Cu(3)	4.359(3)
Cu(2)–O(21)	2.240(2)	Cu(1)···Cu(4)	3.893(3)
Cu(2)–O(22′)	1.950(2)	Cu(1)···Cu(4′)	5.649(3)
Cu(2)–N(1)	2.008(3)	Cu(2)···Cu(3)	5.218(3)
Cu(2)–N(9)	1.958(3)	Cu(2)···Cu(4)	3.612(3)
Cu(3)–O(2)	1.888(2)	Cu(2)···Cu(1′)	4.662(3)
Cu(3)–N(2)	1.984(2)	Cu(2)···Cu(2′)	4.395(3)
Cu(3)–N(3)	2.007(2)	Cu(2)···Cu(4′)	4.760(0)
Cu(3)–N(6)	1.908(3)	Cu(3)···Cu(4)	3.037(1)
Cu(3)–N(6″)	2.906(3)	Cu(3)···Cu(3″)	3.183(3)
Cu(4)–O(2)	1.948(2)	Cu(3)···Cu(4″)	5.028(3)
O(1)–Cu(1)–N(22′)	159.36(9)	Cu(1)–O(1)–Cu(2)	99.64(9)
O(11)–Cu(1)–O(22′)	175.37(9)	Cu(1)–O(22′)–Cu(2)	100.78(9)
O(12)–Cu(1)–N(11′)	141.6(1)	Cu(1)–N(11′)–Cu(4)	101.0(1)
O(1)–Cu(2)–N(9)	158.3(1)	Cu(2)–O(21)–Cu(4)	120.83(9)
O(22′)–Cu(2)–N(1)	158.41(9)	Cu(3)–O(2)–Cu(4)	104.68(9)
O(2)–Cu(3)–N(6)	170.7(1)	Cu(3)–N(3)–Cu(4)	98.2(1)
N(2)–Cu(3)–N(3)	161.9(1)		
O(2)–Cu(4)–N(21)	168.7(1)		
O(21)–Cu(4)–N(3)	175.76(9)		
N(11′)–Cu(4)–N(8″)	167.9(1)		
Cu(1)–O(1)–Cu(2)–O(22′)	10.9(1)	Cu(3)–O(2)–Cu(4)–N(3)	6.8(1)
Cu(3)–N(6)–Cu(3″)–N(6″)	0.00(0)		

[a] Unprimed atoms refer to the crystallographically independent $\{Cu_4\{(py)_2CO_2\}_2(N_3)_3(O_2CMe)\}$ unit, while primed and double primed atoms refer to the head-to-head and tail-to-tail molecular linkages of this unit, respectively.

forming tetranuclear $\{Cu_2\{py)_2C(OH)O\}Cl_3\}_2$ units. The latter are connected at their ends through similar (but not identical) centrosymmetric chloro bridges [Cu(1)–Cl(3)/Cl(3″)–Cu(1′)] linking the tetramers into infinite 1D chains. Both types of the $(\mu$–$Cl)_2$ bridges are asymmetric (see Table 3) and thus the linkages between the dinuclear and the tetranuclear units are weak.

The $(py)_2C(OH)O^-$ group behaves as a tridentate, bis-chelating ligand adopting the η^1:η^2: η^1:μ coordination mode, see Fig. 3. Each pyridyl nitrogen and the deprotonated alkoxide oxygen atom chelate a Cu^{II} center occupying a basal position in the square pyramid. The protonated, free alkoxo arm of the ligand is H-bonded to an oxygen atom of a deprotonated alkoxide arm of another $(py)_2C(OH)O^-$ ligand from an adjacent chain. The three Cl^- ions act as μ ligands. Cl(2), aided by O(1) from the $(py)_2C(OH)O^-$ ligand, link the two Cu^{II} ions that constitute the crystallographically independent unit. Cl(1) and its symmetry related Cl(1′) bridge two dinuclear units to construct the repeating unit of the polymer, $\{Cu_4\{py)_2C(OH)O\}_2Cl_6\}$, whereas Cl(3) and its symmetry related Cl(3″) are responsible for the formation of the chains bridging the tetranuclear units.

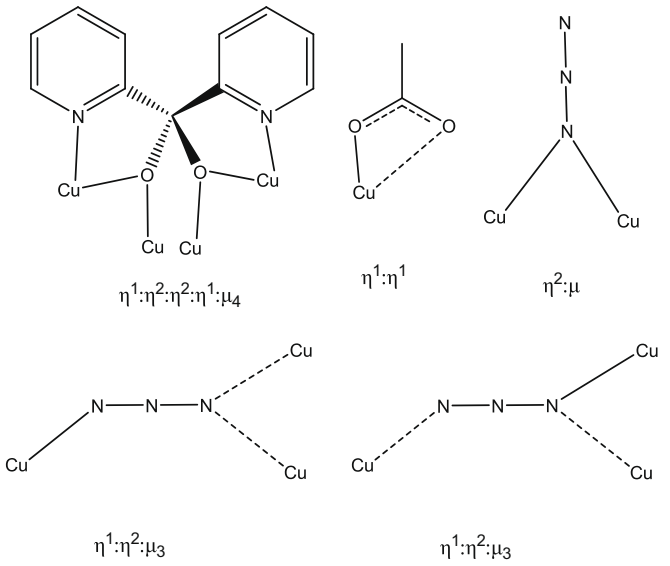

Scheme 2. The coordination modes of the ligands present in complex **1**. The dotted lines indicate weak or very weak coordination bond; the bottom right mode refers to the N(6)N(7)N(8) azido ligand and the bottom left to the N(9) N(10) N(11) ligand.

Complexes **1**–**3** are one-dimensional coordination polymers assembled through weak bonding interactions between well-defined building blocks. A common characteristic in all three complexes is the presence of *interchain* H-bonding interactions, which result in the formation of supramolecular 2D networks (Fig. 4).

In complex **1**·2MeCN·H_2O, the supramolecular interactions are indirect, in the sense that there is no supramolecular contact between the chains. The H-bonding scheme includes a water molecule which is H-bonded to the weakly coordinated oxygen atoms of the two (pseudo)chelating acetate ligands that belong to two neighboring chains. In complexes **2** and **3**, the interactions involve direct H-bonds between two $(py)_2C(OH)O^-$ ligands from different chains. The deprotonated alkoxide arm of *each* ligand is the acceptor, while the protonated oxygen atom is the donor. In that way, a direct linkage between the chains is achieved. A summary of the H-bond dimensions is presented in Table 4.

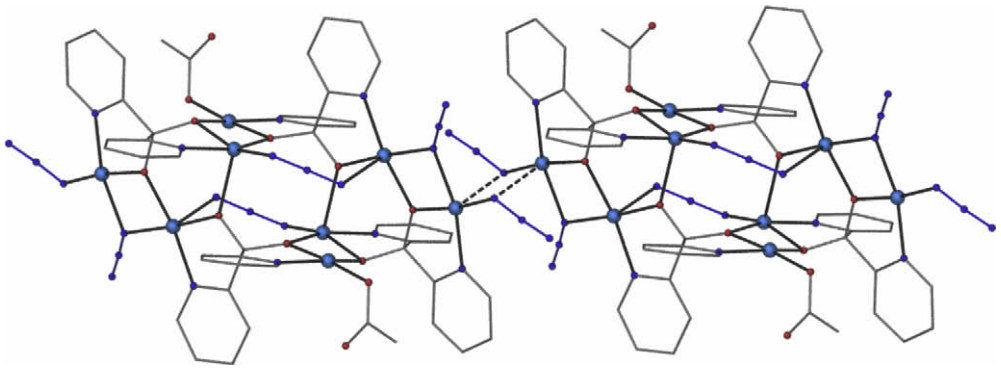

Fig. 2. A sequence of two $[Cu^{II}_8\{(py)_2CO_2\}_4(N_3)_6(O_2CMe)_2]$ cluster units representing a fragment of one infinite molecular chain of the coordination polymer **1**·2MeCN·H_2O. The dashed lines represent the long Cu–N distances. Color code: Cu, sky-blue; C, gray; O, red; N, blue. (For interpretation of the references to color in this figure legend, the reader is referred to the web version of this article.)

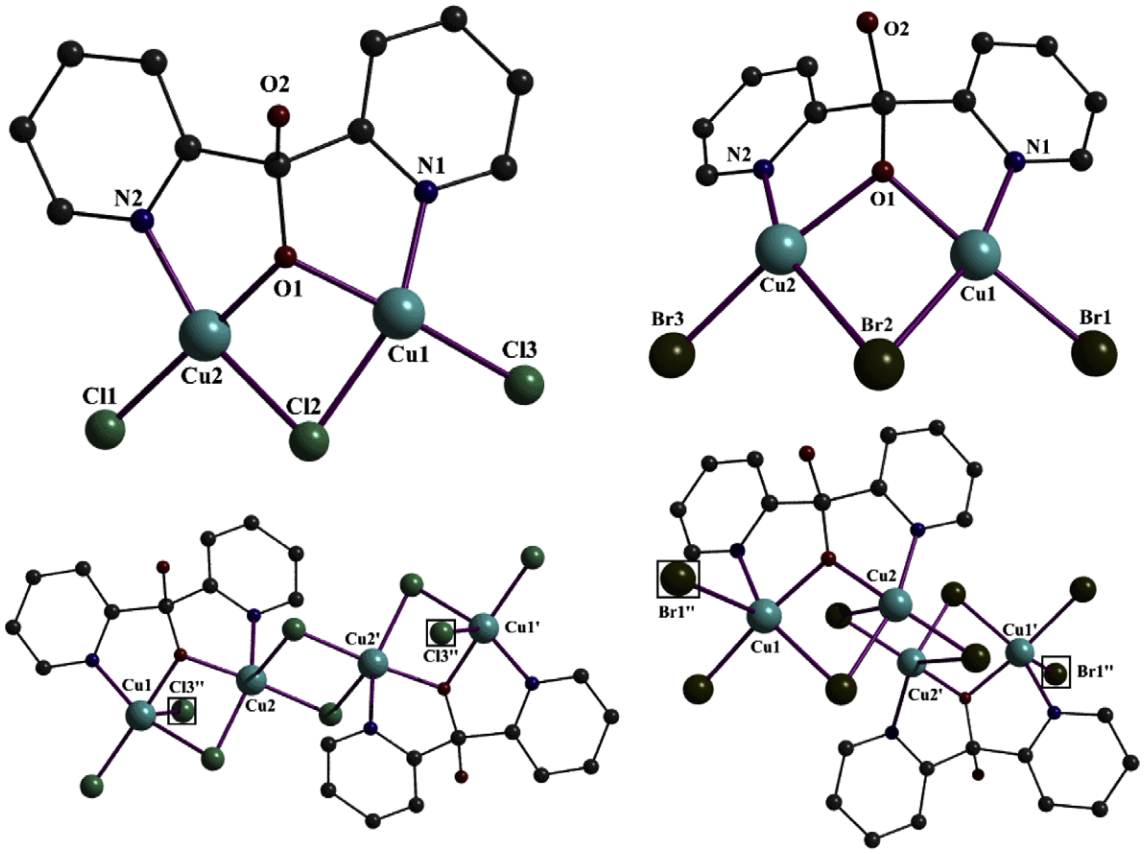

Fig. 3. The crystallographically independent $\{Cu_2\}$ building blocks of the coordination polymers **2** (top left) and **3** (top right). The linkage of the$\{Cu_2\}$ units is achieved through μ–Cl^- or μ–Br^- double bridges towards formation of $\{Cu_4\}$ units, which act as the repeating units present in complexes **2** and **3**. The coordination environment around the Cu^{II} ions is complete only in the pictures of $[Cu_4\{py)_2C(OH)O\}_2X_6]$ (X = Cl, Br), in which the boxed halide groups belong to weakly bonded, adjacent $[Cu_4(py)_2C(OH)O\}_2X_6]$ units. H atoms and solvate molecules are omitted for clarity.

Table 3
Selected interatomic parameters (distances in (Å), angles in (°)) for complexes **2** and **3**.[a]

2		**3**	
Cu(1)–O(1)	1.938(2)	Cu(1)–O(1)	1.950(1)
Cu(1)–N(1)	1.979(2)	Cu(1)–N(1)	1.981(2)
Cu(1)–Cl(3)	2.244(1)	Cu(1)–Br(1)	2.805(0)
Cu(1)–Cl(3″)	2.717(1)	Cu(1)–Br(1″)	2.386(1)
Cu(1)–Cl(2)	2.335(1)	Cu(1)–Br(2)	2.461(1)
Cu(2)–O(1)	1.926(2)	Cu(2)–O(1)	1.936(2)
Cu(2)–N(2)	1.976(2)	Cu(2)–N(2)	1.978(2)
Cu(2)–Cl(1)	2.218(1)	Cu(2)–Br(3)	2.353(1)
Cu(2)–Cl(1′)	2.952(2)	Cu(2)–Br(3′)	3.103(2)
Cu(2)–Cl(2)	2.330(1)	Cu(2)–Br(2)	2.462(1)
Cu(1)···Cu(2)	2.951(1)	Cu(1)···Cu(2)	2.981(1)
Cu(1)···Cu(1″)	3.507(1)	Cu(1)···Cu(1″)	3.591(1)
Cu(2)···Cu(2′)	3.583(1)	Cu(2)···Cu(2′)	4.094(1)
O(1)–Cu(1)–Cl(3)	175.25(7)	O(1)–Cu(1)–Br(1″)	172.43(5)
N(1)–Cu(1)–Cl(2)	153.32(7)	N(1)–Cu(1)–Br(2)	155.57(7)
O(1)–Cu(2)–Cl(1)	173.09(6)	O(1)–Cu(2)–Br(3)	172.49(6)
N(2)–Cu(2)–Cl(2)	162.77(8)	N(2)–Cu(2)–Br(2)	163.84(7)
Cu(1)–O(1)–Cu(2)	99.62(9)	Cu(1)–O(1)–Cu(2)	100.2(1)
Cu(1)–Cl(2)–Cu(2)	78.50(2)	Cu(1)–Br(2)–Cu(2)	74.55(1)
Cu(1)–Cl(3)–Cu(1″)	89.45(3)	Cu(1)–Br(1)–Cu(1″)	87.16(1)
Cu(1)–Cl(3″)–Cu(1″)	89.45(3)	Cu(1)–Br(1′)–Cu(1″)	87.16(1)
Cu(2)–Cl(1)–Cu(2′)	86.50(3)	Cu(2)–Br(3)–Cu(2′)	83.7(1)
Cu(2)–Cl(1′)–Cu(2′)	86.50(3)	Cu(2)–Br(3′)–Cu(2′)	83.7(1)
Cu(1)–O(1)–Cu(2)–Cl(2)	36.8(1)	Cu(1)–O(1)–Cu(2)–Br(2)	39.5(1)
Cu(1)–Cl(3)–Cu(1″)–Cl(3″)	0.00(0)	Cu(1)–Br(1)–Cu(1″)–Br(1″)	0.00(0)
Cu(2)–Cl(1)–Cu(2′)–Cl(1′)	0.00(0)	Cu(2)–Br(3)–Cu(2′)–Br(3′)	0.00(0)

[a] Unprimed atoms refer to the crystallographically independent $\{Cu_2\{(py)_2C(OH)O\}X_3\}$ unit, while primed and double primed atoms refer to the interdimer and intertetramer molecular linkages of this unit, respectively.

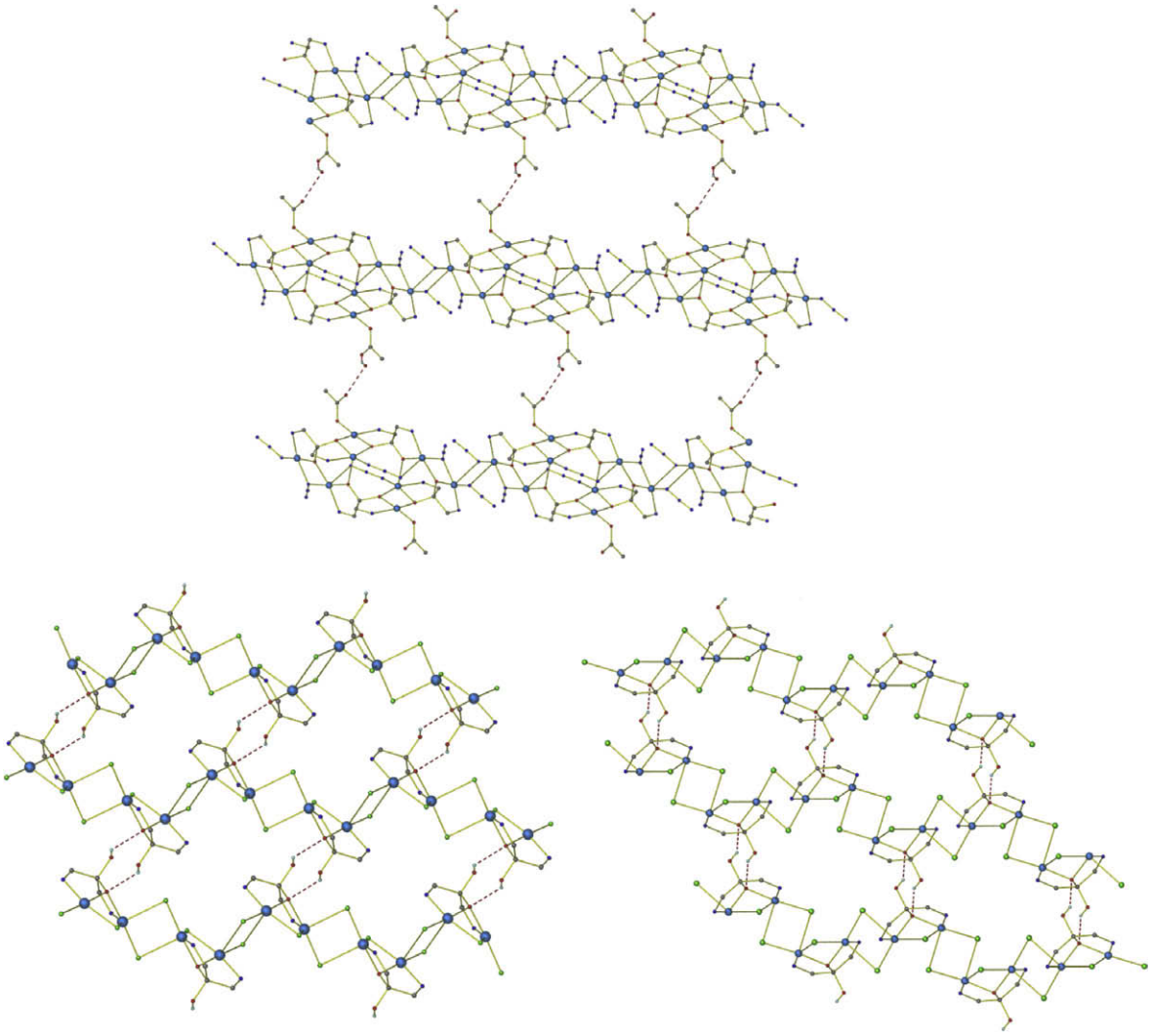

Fig. 4. The 2D supramolecular sheets for complex **1** (top), and complexes **2** (bottom left) and **3** (bottom right). Color code: Cu, sky-blue; C, gray; O, red; N, blue; halide, green; hydrogen, cyan. (For interpretation of the references to color in this figure legend, the reader is referred to the web version of this article.)

3.3. Magnetic properties

Solid-state, dc magnetic susceptibility measurements were performed on polycrystalline samples of complexes **1**–**3** in the temperature range 2.0–300 K. Data are shown in Figs. 5 and 6.

Compound **1** shows a $\chi_M T$ value at room temperature of 2.49 $cm^3\ mol^{-1}$ K, clearly lower than the expected for eight $S = ½$ centers (3.00 $cm^3\ mol^{-1}$ K for $g = 2.00$). Upon cooling, the $\chi_M T$ value decreases continuously, tending to zero at low temperature. The χ_M versus T plot exhibits a maximum at 120 K, indicating an overall antiferromagnetic interaction. Fit of the experimental data was performed on the basis of a detailed analysis of the structural data. Each octanuclear repeating unit of compound **1** contains four dinuclear subunits linked by long (Jahn–Teller) contacts. Two of these subunits contain two alkoxo bridges each giving a Cu_2O_2

Table 4
Intrerchain hydrogen bonding interactions for complexes **1**–**3**.[a]

D–H···A	D···A (Å)	H···A (Å)	DHA (°)
Complex ***1***			
$O(H_2O)$–H···$O(O_2CMe)$	2.694 2.877	1.730	165.4
Complex ***2***			
$O\{(py)_2C(OH)O\}$–H···$O\{(py)_2C(OH)O\}$	3.057	2.493	136.1
Complex ***3***			
$O\{(py)_2C(OH)O\}$–H···$O\{(py)_2C(OH)O\}$	3.042	2.393	146.0

[a] A = acceptor; D = donor.

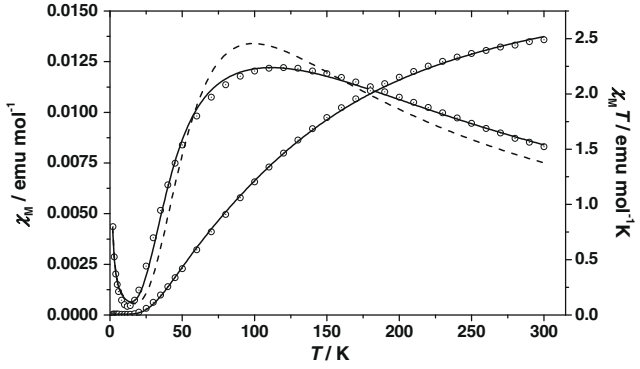

Fig. 5. χ_M and $\chi_M T$ vs. T plots for compound **1**. Solid lines show the best fit simulation of the experimental data by using two independent J coupling constants. The dashed line shows the best fit simulation assuming a mean J value (see text).

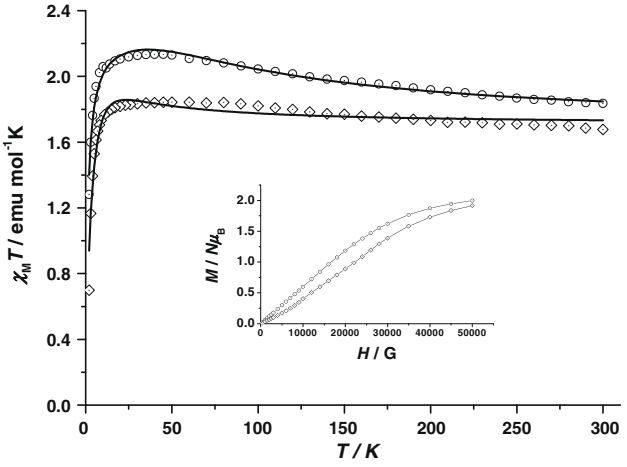

Fig. 6. $\chi_M T$ vs. T for compounds **2** (dot-centered circles) and **3** (dot-centered rhombs). Solid lines show the best fit simulation of the experimental data (see text). The magnetization plots for compounds **2** and **3** are shown in the inset.

ring, while each of the other two has an asymmetric alkoxo/end-on azido bridge creating a Cu_2NO ring. The susceptibility plots indicate a moderately strong antiferromagnetic coupling and a response close to diamagnetism at low temperature. A first attempt to fit the experimental data was made assuming one mean value for all the dinuclear subunits and neglecting the weak inter- or intramolecular interactions related to the axial-equatorial/basal interactions, which are operative only at very low temperatures. Applying the conventional expression derived from the Hamiltonian $H = -JS_1S_2$, including a term to evaluate the paramagnetic impurities, gives a non-acceptable simulation with the best-fit parameters $J = -111\ cm^{-1}$, $g = 1.88\%$ and 0.2% of paramagnetic impurities, see the dashed line in Fig. 5.

This result suggests that the one-J model is oversimplified and at least two different coupling constants should be applied in order to try to differentiate the two independent kinds of dinuclear subunits. Assuming two dinuclear subunits with an equal contribution of 50% for each to the total susceptibility value gives an excellent fit with best-fit parameters $J_1 = -88.0(6)\ cm^{-1}$, $J_2 = -227(7)\ cm^{-1}$, $g = 2.08(2)\%$ and 0.26(1)% of paramagnetic impurities, see the solid lines in Fig. 5.

The dinuclear Cu_2O_2 subunits, with Cu–O–Cu bond angles of around 100° should exhibit a clear antiferromagnetic response, whereas the alkoxo/azido-bridged subunits have two ligands that tend to mediate a ferromagnetic interaction (end-on azido, Cu–N–Cu bond angle of 98.2°) and an antiferromagnetic coupling (alkoxo, Cu–O–Cu bond angle of 104.6°). The problem of mixed alkoxo/end-on azido bridges was studied by Kahn and co-workers [2a–c] and by other scientists [2d–f] who showed that antiferromagnetic J values around $-100\ cm^{-1}$ are common. Based on those studies, we can unambiguously assign J_1 to the alkoxo/azido-bridged subunits and J_2 to the Cu_2O_2 subunits.

Compounds **2** and **3** show $\chi_M T$ values at room temperature of 1.84–1.68 $cm^3\ mol^{-1}\ K$, respectively, slightly higher than the expected value for four $S = ½$ centers ($1.50\ cm^3\ mol^{-1}\ K$ for $g = 2.00$). Upon cooling, the $\chi_M T$ values increase giving rounded maxima below 50 K and tend to zero at very low temperatures. The continuous increase of $X_M T$ down to 50 K suggests a ferromagnetic component in the overall magnetic behavior of the two compounds.

From structural data, the stronger interactions for both complexes should be mediated by the alkoxide/halide bridges, whereas a weak interaction would be expected for the axial–basal double halide bridges. The fit was performed applying the conventional expression derived from the Hamiltonian $H = -JS_1S_2$, in which J is related to the interaction mediated by the alkoxo/halide bridge, and introducing a Θ term that takes into consideration the low temperature effects (interdimer or anisotropic effects). Best-fit parameters of the experimental data are $J = +90(7)\ cm^{-1}$, $g = 2.124(8)$, $\Theta = -1.22(6)\ K$ for **2** and $J = +21(3)\ cm^{-1}$, $g = 2.13(1)$ and $\Theta = -2.8(1)\ K$ for **3**.

Magnetization experiments performed at 2 K show a slightly sigmoid plot for both compounds (inset of Fig. 6). The magnetization value tends to the equivalent of two electrons per dinuclear unit, as can be expected from the dominant ferromagnetic interaction. From susceptibility data, the ground state for compounds **2** and **3** should be $S = 1$ for each dinuclear subunit. In good agreement, the magnetization tends to two electrons. Comparison with the expected Brillouin plot for $S = 1$ does not fit properly the experimental data because of the weak interdimer interactions that modify the shape of the magnetization, which is slightly sigmoidal. First derivative exhibits a broad maximum around 10 000 G ($1\ cm^{-1}$ approximately), which should be attributed to the sum of low temperature effects (mainly interdimer interactions but also weak intermolecular interactions or anisotropic effects).

The positive sign of the dominant interactions for **2** and **3** is becoming the most interesting feature of the above results. As can be seen in Table 5, moderate or strong antiferromagnetic interactions characterize the magnetic response of Cu^{II} pairs bridged by alkoxo/halide ligands. When the Cu_2XO four-membered ring is close to planarity, the Cu–O–Cu bond angle is larger than 110° and in all cases good overlap of the Cu^{II} magnetic orbital with the orbitals of both bridging atoms gives strong antiferromagnetic

Table 5
Bond parameters and magnetic exchange interaction for several Cu^{II} pairs with alkoxo/halide bridges.[a]

Compound[b]	Dihedral Cu(1)–O–X/O–X–Cu(2) angle[a]	Cu–O–Cu	Cu–X–Cu	$J\ (cm^{-1})$	Ref.
FESJIW[c]	178.1°	111.4°	89.6°	−335	[25]
FOGGIR[c]	172.5°	113.4	86.1°	−443	[26]
JEDFUU[c]	173.5°	112.8°	87.8°	−348	[27]
OBOWUY[c]	172.0°	115.7°	84.8°	−374	[28]
WAHSOO[c]	165.0°	112.4°	81.8°	−177	[29]
TOGLAC[c]	141.9°	101.9°	81.0°	0	[16a]
TOGLEG[c]	134.4°	97.3°	78.4°	+71	[16b]
Compound **2**[c]	134.5°	99.6°	78.5°	+90	This work
FESJUI[d]	180°	114.6°	84.8°	−335	[26]
WAHSUU[d]	171.3°	115.3°	79.3°	−219	[29]
Compound **3**[d]	131.8°	100.2	74.6°	+21	This work

[a] The Cu^{II} ions are 5-coordinate.
[b] The codes refer to the CCDC data base.
[c] X = Cl.
[d] X = Br.

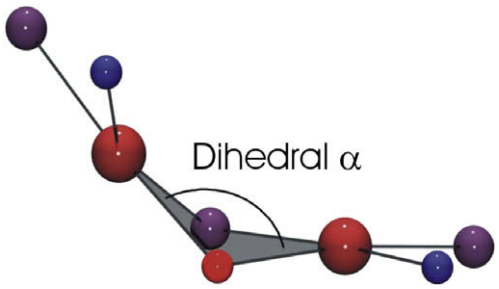

Scheme 3. Cu(1)–O–X/O–X–Cu(2) dihedral angle, see text.

interactions. In contrast, compounds **2** and **3** are folded showing small dihedral angles between the Cu(1)–O(1)–Cl(2) and O(1)–Cl(2)–Cu(2) planes of 134.5° and 131.8°, respectively, Scheme 3. When the dihedral angle *a* decreases, both Cu–O–Cu and Cu–X–Cu bond angles also decrease, reaching values of around 100° and <80° for compounds **2** and **3**. These lower bond angles, together with the worse overlap involving the in-plane orbitals of the bridges reduce the antiferromagnetic component of the coupling, and the experimental response is becoming ferromagnetic. Compound TOGLEG is very similar to compound **2**. Our compounds have similar bond parameters showing a clear ferromagnetic behavior. From the above discussion, it is becoming clear that the deviation from planarity of such Cu_2XO rings reduces the antiferromagnetic response and for large deviations from 180° (small dihedral angles α) these systems can reach a dominant ferromagnetic response.

4. Conclusions

The synthesis, crystallographic characterization and interpretation of the magnetic properties of three 1D Cu^{II} coordination polymers featuring the *gem*-diolate forms of di-2-pyridyl ketone have been reported. Complexes **1**–**3** are based on tetranuclear (**1**) or dinuclear (**2**, **3**) units linked through the organic ligand, while the N_3^- or X^- (X=Cl, Br) groups assemble these units into infinite coordination polymers. Additionally, the presence of H-bonding between the polymeric chains increases their dimensionality through supramolecular interactions giving rise to 2D layers. The magnetic study of the compounds was carried out taking into account only the dominant exchange interactions within the dinuclear subunits/units. The weaker exchange coupling interactions between the dinuclear moieties could not be modelled, since the intradinuclear coupling appears to be much stronger than the interdinuclear one, a fact that renders the estimation of the numerical values of the latter difficult. The intradinuclear exchange interactions have been found to vary from strongly and moderately antiferromagnetic in complex **1** to moderately ferromagnetic in complexes **2** and **3**. Overall, this works expands the chemistry of the $Cu^{II}/(py)_2CO$ reaction systems and adds three new polymeric compounds in the growing family of Cu^{II} complexes with the derivatives of the $(py)_2CO$ ligand.

Supplementary data

CCDC 730699, 730700, 7307011 contains the supplementary crystallographic data for **1**·2MeCN·H_2O, **2** and **3**. These data can be obtained free of charge via http://www.ccdc.cam.ac.uk/conts/retrieving.html, or from the Cambridge Crystallographic Data Centre, 12 Union Road, Cambridge CB2 1EZ, UK; fax: (+44) 1223-336-033; or e-mail: deposit@ccdc.cam.ac.uk.

References

[1] B. Le Guennic, S. Petit, G. Chastanet, G. Pilet, D. Luneau, N. Ben Amor, V. Robert, Inorg. Chem. 47 (2008) 572.
[2] (a) T. Mallah, M.L. Boillot, O. Kahn, J. Gouteron, S. Jeannin, Y. Jeannin, Inorg. Chem. 25 (1986) 3058;
(b) T. Mallah, O. Kahn, J. Gouteron, S. Jeannin, Y. Jeannin, C.J. O'Connor, Inorg. Chem. 26 (1987) 1375;
(c) O. Kahn, T. Mallah, J. Gouteron, S. Jeannin, Y. Jeannin, J. Chem. Soc., Dalton Trans. (1989) 1117;
(d) A. Benzekri, P. Dubourdeaux, J.M. Latour, J. Laugier, P. Rey, Inorg. Chem. 27 (1988) 3710;
(e) T. Chattopadhyay, K.S. Banu, A. Banerjee, J. Ribas, A. Majee, M. Nethaji, D. Das, J. Mol. Struct. 833 (2007) 13;
(f) P. Chaudhuri, R. Wagner, T. Weyhermüller, Inorg. Chem. 46 (2007) 5134.
[3] J. Yoon, E.I. Solomon, Coord. Chem. Rev. 251 (2007) 379.
[4] (a) T. Glaser, M. Heidemeier, J.B.H. Strautmann, H. Bögge, A. Stammler, E. Krickemeyer, R. Huenerbein, S. Grimme, E. Bothe, E. Bill, Chem. Eur. J. 13 (2007) 9191;
(b) B. Sarkar, M.S. Ray, Y.-Z. Li, Y. Song, A. Figuerola, E. Ruiz, J. Cirera, J. Cano, A. Ghosh, Chem. Eur. J. 13 (2007) 9297.
[5] (a) M. Casarin, C. Corvaja, C. Di Nicola, D. Falcomer, L. Franco, M. Monari, L. Pandolfo, C. Pettinari, F. Piccinelli, Inorg. Chem. 44 (2005) 6265;
(b) Y.-Z. Zhang, H.-Y. Wei, F. Pan, Z.-M. Wang, Z.-D. Chen, Song Gao, Angew. Chem., Int. Ed. 44 (2005) 5841;
(c) W. Ouellette, A.V. Prosvirin, V. Chieffo, K.R. Dunbar, B. Hudson, J. Zubieta, Inorg. Chem. 45 (2006) 9346;
(d) C. Yuste, A. Bentama, S.-E. Stiriba, D. Armentano, G. De Munno, F. Lloret, M. Julve, Dalton Trans. (2007) 5190;
(e) K.C. Mondal, P.S. Mukherjee, Inorg. Chem. 47 (2008) 4215;
(f) C.-D. Wu, L. Ma, W. Lin, Inorg. Chem. 47 (2008) 11446;
(g) S.-B. Ren, X.-L. Yang, J. Zhang, Y.-Z. Li, Y.-X. Zheng, H.-B. Du, X.-Z. You, Cryst. Eng. Commun. (2009) 246.
[6] (a) P. Klüfers, J. Schuhmacher, Angew. Chem., Int. Ed. 34 (1995) 2119;
(b) L.N. Dawe, L.K. Thompson, Angew. Chem., Int. Ed. 46 (2007) 7440;
(c) J. He, J.-X. Zhang, C.-K. Tsang, Z. Xu, Y.-G. Yin, D. Li, S.-W. Ng, Inorg. Chem. 47 (2008) 7948;
(d) T. Shiga, K. Maruyama, L. Han, H. Oshio, Chem. Lett. 34 (2005) 1648;
(e) M. Murugesu, R. Clérac, C.E. Anson, A.K. Powell, Chem. Commun. (2004) 1598;
(f) M. Murugesu, R. Clérac, C.E. Anson, A.K. Powell, Inorg. Chem. 43 (2004) 7269.
[7] Y.-M. Li, J.-L. Zhang, X.-W. Zhao, Acta Crystallogr. E63 (2007) m1510.
[8] Y.-M. Li, J.-J. Zhang, R.-B. Fu, S.-C. Xiang, T.-L. Sheng, D.-Q. Yuan, X.-H. Huang, X.-T. Wu, Polyhedron 25 (2006) 1618.
[9] (a) P.J. Steel, C.J. Sumby, Dalton Trans. (2003) 4505;
(b) T.C. Stamatatos, V. Tangoulis, C.P. Raptopoulou, A. Terzis, G.S. Papaefstathiou, S.P. Perlepes, Inorg. Chem. 47 (2008) 7969.
[10] V. Tangoulis, C.P. Raptopoulou, S. Paschalidou, E.G. Bakalbassis, S.P. Perlepes, A. Terzis, Angew. Chem., Int. Ed. 36 (1997) 1083.
[11] (a) V. Tangoulis, C.P. Raptopoulou, A. Terzis, S. Paschalidou, S.P. Perlepes, E.G. Bakalbassis, Inorg. Chem. 36 (1997) 3996;
(b) M.-L. Tong, H.K. Lee, Y.-X. Tong, X.-M. Chen, T.C.W. Mak, Inorg. Chem. 39 (2000) 4666.
[12] .E. Sheng, W. Yu, X. Li, Inorg. Chem. Commun. 11 (2008) 418.
[13] S.R. Breeze, S. Wang, J.E. Greedan, N.P. Raju, Inorg. Chem. 35 (1996) 6944.
[14] J.M. Seco, M. Quirós, M.J. González Garmendia, Polyhedron 19 (2000) 1005.
[15] (a) J. Manzur, A.M. Garcia, M.T. Garland, V. Acuña, O. Gonzalez, O. Peña, A.M. Atria, E. Spodine, Polyhedron 15 (1996) 821;
(b) V. Tangoulis, C.P. Raptopoulou, S. Paschalidou, A.E. Tsohos, E.G. Bakalbassis, A. Terzis, S.P. Perlepes, Inorg. Chem. 36 (1997) 5270;
(c) D.-Y. Wu, W. Huang, W.-J. Hua, Y. Song, C.-Y. Duan, S.-H. Li, Q.-J. Meng, Dalton Trans. (2007) 1838.
[16] (a) A.C. Deveson, S.L. Heath, C.J. Harding, A.K. Powell, J. Chem. Soc., Dalton Trans. (1996) 3173;
(b) A.N. Papadopoulos, V. Tangoulis, C.P. Raptopoulou, A. Terzis, D.P. Kessissoglou, Inorg. Chem. 35 (1996) 559;
(c) C.-M. Liu, D.-Q. Zhang, D.-B. Zhu, Inorg. Chim. Acta 362 (2009) 1383.
[17] (a) G.S. Papaefstathiou, S.P. Perlepes, Comments Inorg. Chem. 23 (2002) 249;
(b) T.C. Stamatatos, C.G. Efthymiou, C.C. Stoumpos, S.P. Perlepes, Eur. J. Inorg. Chem. (Microreview), in press.
[18] Rigaku/MSC, CRYSTALCLEAR, Rigauk/MSC Inc., The Woodlands, Texas, USA, 2005.
[19] G.M. Sheldrick, SHELXS-97, Structure Solving Program, University of Göttingen, Germany, 1997.
[20] G.M. Sheldrick, SHELXL-97, Crystal Structure Refinement Program, University of Göttingen, Germany, 1997.
[21] C.C. Stoumpos, I.A. Gass, C.J. Milios, N. Lalioti, A. Terzis, G. Aromi, S.J. Teat, E.K. Brechin, S.P. Perlepes, Dalton Trans. (2008) 307.
[22] C.C. Stoumpos, A. Escuer, S.P. Perlepes, in preparation.
[23] (a) A. Tsohos, S. Dionyssopoulou, C.P. Raptopoulou, A. Terzis, E.G. Bakalbassis, S.P. Perlepes, Angew. Chem., Int. Ed. 38 (1999) 983;
(b) G.S. Papaefstathiou, S.P. Perlepes, A. Escuer, R. Vicente, M. Font-Bardia, X. Solans, Angew. Chem., Int. Ed. 40 (2001) 884;
(c) G.S. Papaefstathiou, A. Escuer, R. Vicente, M. Font-Bardia, X. Solans, S.P. Perlepes, Chem. Commun. (2001) 2414;
(d) A.K. Boudalis, Y. Sanakis, J.M. Clemente-Juan, B. Donnadieu, V.

Nastopoulos, A. Mari, Y. Coppel, J.-P. Tuchagues, S.P. Perlepes, Chem. Eur. J. 14 (2008) 2514.
[24] J.L. Manson, H.I. Southerland, B. Twamley, R. Rai, J.L. Musfeldt, Dalton Trans. (2008) 5655.
[25] K.D. Karlin, A. Farooq, J.C. Hayes, B.I. Cohen, T.M. Rowe, E. Sinn, J. Zubieta, Inorg. Chem. 26 (1987) 1271.
[26] A. Benzekri, P. Dubourdeaux, J.M. Latour, J. Laugier, P. Rey, Chem. Commun. (1987) 1564.
[27] G.A. van Albada, I. Mutikainen, U. Turpeinen, J. Reedijk, Polyhedron 25 (2006) 81.
[28] S.P. Foxon, D. Utz, J. Astner, S. Schindler, F. Thaler, F.W. Heinemann, G. Liehr, J. Mukherjee, V. Balamurugan, D. Ghosh, R. Mukherjee, Dalton Trans. (2004) 2321.
[29] I.A. Koval, M. Huisman, A.F. Stassen, P. Gamez, O. Roubeau, C. Belle, J.L. Pierre, E. Saint-Aman, M. Lüken, B. Krebs, M. Lutz, A.L. Spek, J. Reedijk, Eur. J. Inorg. Chem. (2004) 4036.